Effects of magnetic perturbations on axisymmetric divertors

Alkesh Punjabi[1], Allen Boozer[2]

[1]*Hampton University, Hampton, VA 23668, USA*

[2]*Columbia University, New York, NY 10227, USA*

When the nested magnetic surfaces that confine a non-axisymmetric plasma have an outermost surface that is well separated from the walls, then the plasma reaches the surrounding walls along magnetic flux tubes that are defined by turnstiles in cantori. An analytic model is derived in which the width and nature of the intersection of points of magnetic flux tubes can be studied. This exact model is based on the Boozer-Rechester two wire model [A. H. Boozer and A. B. Rechester, Phys. Fluids **21**, 682 (1978)]. Boozer and Rechester represented the magnetic field using the complete elliptic integrals and the Jacobi elliptic functions, but they did not place the equations in terms of an explicit magnetic field line Hamiltonian. In our model this is done and the magnetic field lines are modified by the addition of a fixed small radial spiraling velocity. The lines eventually cross the outermost confining magnetic surface and form flux tubes that strike the surrounding walls. The width and nature of the intersection of points of these flux tubes are studied in the limit as the spiraling velocity vanishes. This is done for both an axisymmetric divertor and for an axisymmetric divertor subjected to a quadrupole perturbation that has an orientation that rotates with the toroidal angle. The scaling with the spiraling velocity of the loss time and size of the intersection region give the important information on the topology of the magnetic field lines, which determines the plasma-exhaust properties of a divertor. Some of these topological features appear to have a universal scaling.

Two wire model of Boozer and Rechester [1] is used to calculate the poloidal flux ψ_p in axisymmetric divertor with quadrupole magnetic perturbation. Poloidal flux is Hamiltonian for the trajectories of magnetic field lines. From the expression for the poloidal flux the equations for the trajectories of magnetic field line in axisymmetric divertor are derived for regions inside the separatrix, outside the separatrix, and with and without exact quadrupole perturbation [2]. These equations involve complete elliptical integrals $K(k)$ and $E(k)$ and Jacobi elliptic functions sn, dn, and cn. A rather unusual choice for the magnetic angle θ is made to circumvent the jump in magnetic angle outside the separatrix. Full details are given in [2]. The basic geometry of the model is shown in Figure 1. $N_0 = 3600$ field lines are started on the starting surface, Figure 3 and integrated for 10,000 toroidal circuits. The strike points on the three walls (Figure 3) are calculated. Field lines are given a radial velocity u_ψ.

u_ψ is normalized to the toroidal flux ψ_s enclosed by separatrix. u_ψ/ψ_s is varied from 1E-2, 9E-3, 8E-3,…,1E-6 per radian of toroidal advance. The number of lines that have not struck the walls is $N_B(\varphi)$. φ is the toroidal angle. φ_0 is the toroidal angle when the first line strikes the walls. φ_{LOSS} is the toroidal advance after φ_0 when $N_B(\varphi)/N_0 = 1/e$.

This paper investigates how the magnetic flux in magnetic turnstiles escapes by threading through infinite Markov chain of cantori in axisymmetric divertors [3]. This is an extremely complicated process. The simulation methodology developed for the study quantifies the process in terms of scaling laws for φ_0, φ_{LOSS}, and $N_B(\varphi)$ with u_ψ in the limit as $u_\psi \to 0$. Scaling laws are calculated from the simulations for unperturbed axisymmetric divertor and for perturbed axisymmetric divertor when the exact quadrupole perturbation is high. Preliminary results of study are reported.

Width of stochastic layer: When an axisymmetric divertor is perturbed, the width of the strike points on the wall has a sharp change in scaling at the perturbation amplitude of $\delta = 2 \times 10^{-4}$, Figure 4. The region of $\delta > 2 \times 10^{-4}$ is the high perturbation region and the region $\delta < 2 \times 10^{-4}$ is the low perturbation region.

Unperturbed axisymmetric divertor: For unperturbed axisymmetric divertor, φ_0 scales as $1/u_\psi$, Figure 5. φ_{LOSS} scales as $\exp(-\text{constant} \cdot u_\psi)$ for the wall inside the upper lobe (wall 1); φ_{LOSS} is roughly constant for $u_\psi < 10^{-3}$ and again constant for $u_\psi > 10^{-3}$ for wall through the X-point (wall 2); and φ_{LOSS} scales as u_ψ to the power -5/3 for the wall in lower lobe (wall 3). See Figure 6. $N_B(\varphi)/N_0$ scales as $g_1 \psi_0 \ln(p)/u_\psi$ where g_1 is a universal constant independent of u_ψ and $g_1 \approx -1/3$ for all three walls, Figures 7 and 8.

Perturbed axisymmetric divertor – High perturbation: Amplitude of quadrupole perturbation is chosen to be $\delta = 10^{-3}$. φ_0 scales as $1/u_\psi$ for all three walls. φ_{LOSS} scales as u_ψ to the power -6/5 for wall 1 and power -4/5 for walls 2 and 3, Figure 10. $N_B(\varphi)/N_0$ scales as $\exp\left[((\phi - \phi_0)/\phi_{LOSS})^p \right]$ with the power p in exponent $p = 2$ for all three walls in the limit as $u_\psi \to 0$; Figure 11.

Perturbed axisymmetric divertor – Low perturbation: Amplitude of quadrupole perturbation is chosen to be $\delta = 10^{-4}$. φ_0 scales as $1/u_\psi$ for all three walls. φ_{LOSS} scales as u_ψ to the power -4/5 for wall 1 and power -1/2 for walls 2 and 3, Figure 12. $N_B(\varphi)/N_0$ scales as $\exp\left[((\phi - \phi_0)/\phi_{LOSS})^p \right]$ with the power p in the exponent $p = 3$ for all three walls in the limit $u_\psi \to 0$; Figures 13.
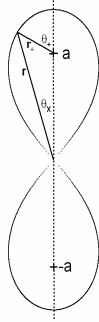
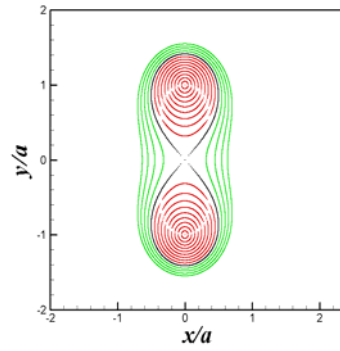Fig. 1: The basic geometry of the two wire model.

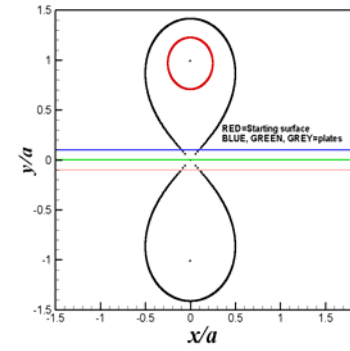Fig. 2: The equilibrium magnetic surfaces.

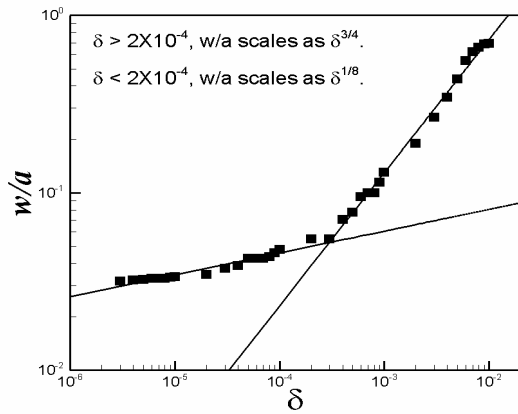Fig. 3: The starting surface and the intercepting planes.

Fig. 4: The width w of stochastic layer as a function of amplitude δ of the quadrupole perturbation.
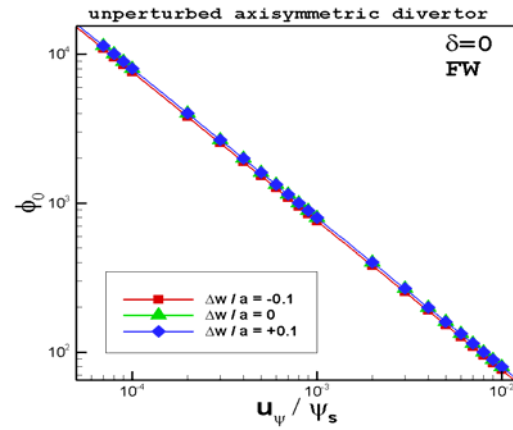

Fig. 5: Scaling of φ_0 with u_ψ for unperturbed axisymmetric divertor.
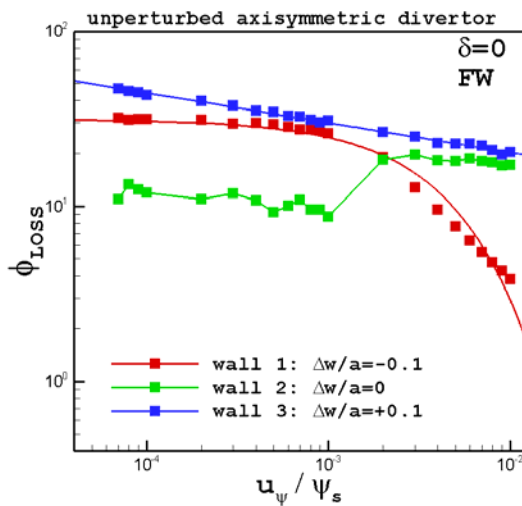
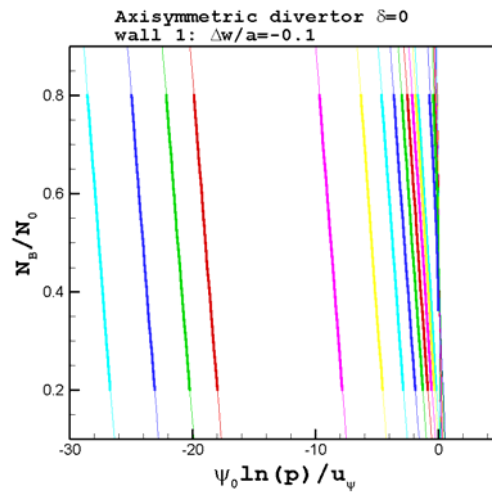Fig. 6: Scaling of φ_{LOSS} with u_ψ for unperturbed axisymmetric divertor; wall 1 (red), wall 2 (green), wall 3 (blue).

Fig. 7:$N_B(\varphi)/N_0$ vs $\psi_0 \ln(p)/u_\psi$ for wall 1for u_ψ/ψ_s = 1E-2,9E-3,…,7E-5.

3

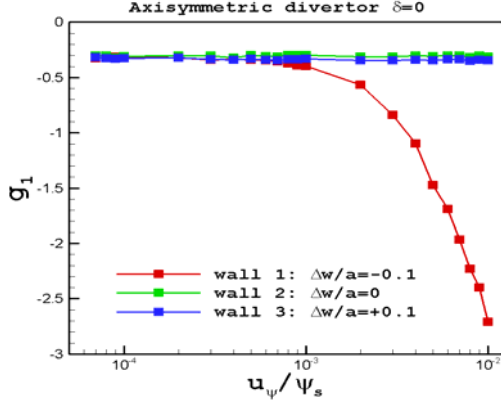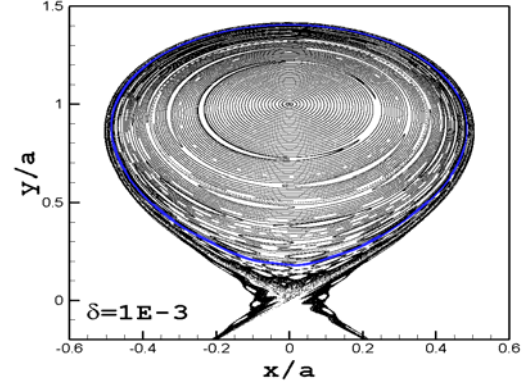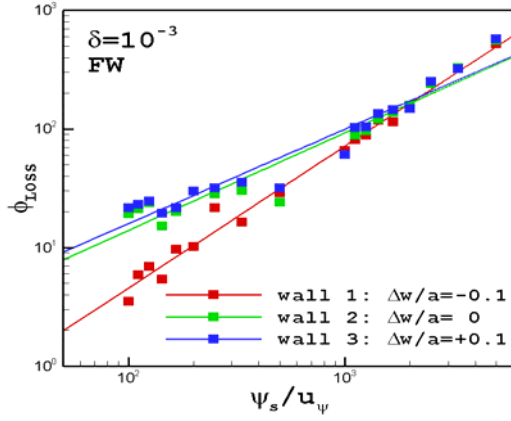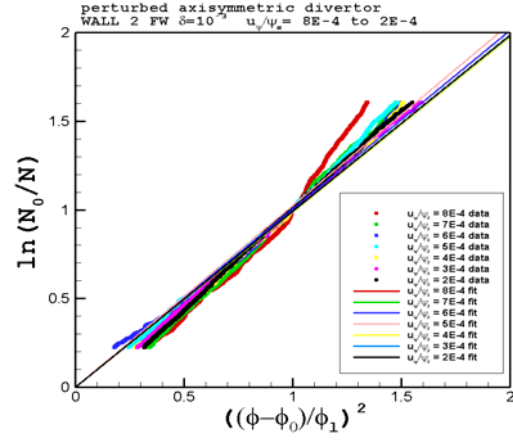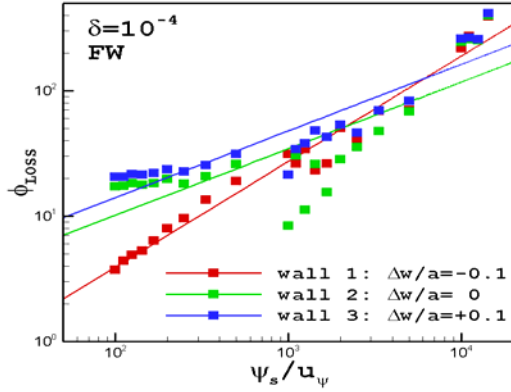Fig. 8: The universal constant g_1 for scaling of $N_B(\varphi)$.

Fig. 9: Phase portrait of the perturbed axisymmetric divertor for high perturbation.

Fig. 10: Scaling of Φ_{LOSS} for perturbed axisymmetric divertor; wall 1 (red), wall 2 (green), wall 3 (blue).

Fig. 11: Scaling of $N_B(\varphi)$ for wall 2 for high perturbation in the limit $u_\psi \to 0$.

Fig. 12: Scaling of Φ_{LOSS} for perturbed axisymmetric divertor; wall 1 (red), wall 2 (green), wall 3 (blue).
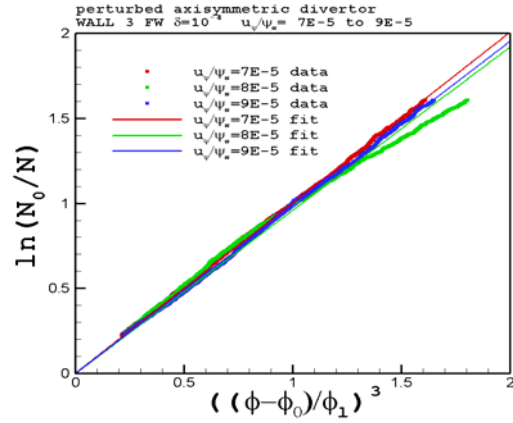
Fig. 13: Scaling of $N_B(\varphi)$ for wall 3 for low perturbation in the limit $u_\psi \to 0$.

[1] A. H. Boozer and A. B. Rechester, Phys. Fluids **21**, 682 (1978).
[2] Simulation of stellarator divertors, A. H. Boozer and A. Punjabi, submitted for publication.
[3] A. H. Boozer and A. Pujabi, Phys. Plasmas **23**, 102513 (2016).

4